Available online at www.sciencedirect.com
ScienceDirect
European Journal of Pharmaceutics and Biopharmaceutics 68 (2008) 513–525
European Journal of Pharmaceutics and Biopharmaceutics
www.elsevier.com/locate/ejpb

Research paper

Chitosan–sodium alginate nanoparticles as submicroscopic reservoirs for ocular delivery: Formulation, optimisation and *in vitro* characterisation

Sanjay K. Motwani *, Shruti Chopra, Sushma Talegaonkar, Kanchan Kohli, Farhan J. Ahmad, Roop K. Khar

Department of Pharmaceutics, New Delhi, India

Received 1 January 2007; accepted in revised form 18 September 2007
Available online 25 September 2007

Abstract

Management of extraocular disease is mainly limited by the inability to provide long-term extraocular drug delivery without avoiding the systemic drug exposure and/or affecting the intraocular structures and poor availability of drugs, which may be overcome by prolonging the contact time with the ocular surface, for instance with bioadhesive polymers. In the present study, mucoadhesive chitosan (CS)-sodium alginate (ALG) nanoparticles were investigated as a new vehicle for the prolonged topical ophthalmic delivery of antibiotic, gatifloxacin. A modified coacervation or ionotropic gelation method was used to produce gatifloxacin-loaded submicroscopic nanoreservoir systems. It was optimised using design of experiments by employing a 3-factor, 3-level Box-Behnken statistical design. Independent variables studied were the amount of the bioadhesive polymers: CS, ALG and the amount of drug in the formulation. The dependent variables were the particle size, zetapotential, encapsulation efficiency and burst release. Response surface plots were drawn, statistical validity of the polynomials was established and optimised formulations were selected by feasibility and grid search. Nanoparticles were characterised by FT-IR, DSC, TEM and atomic force microscopy. Drug content, encapsulation efficiency and particle properties such as size, size distribution (polydispersity index) and zetapotential were determined. The designed nanoparticles have average particle size from 205 to 572 nm (polydispersity from 0.325 to 0.489) and zetapotential from 17.6 to 47.8 mV. Nanoparticles revealed a fast release during the first hour followed by a more gradual drug release during a 24-h period following a non-Fickian diffusion process. Box-Behnken experimental design thus facilitated the optimisation of mucoadhesive nanoparticulate carrier systems for prolonged ocular delivery of the drug.

Keywords: Optimisation; Response surface methodology; Box-Behnken design; Formulation; Mucoadhesion; Nanoparticles

1. Introduction

One of the most attractive areas of research in drug delivery today is the design of nanosystems that are able to deliver drugs to the right place, at appropriate times and at the right dosage. These nanocarriers are submicron particles containing entrapped drugs intended for enteral or parenteral administration, which may prevent or minimise the drug degradation and metabolism as well as cellular efflux [1,2]. Nanoparticles also have a long shelf-life, have been made of safe materials, including synthetic biodegradable polymers, natural biopolymers, lipids and polysaccharides and have the potential for overcoming important mucosal barriers, such as the intestinal, nasal and ocular barriers [3].

Major problem encountered with the conventional topical delivery of ophthalmic drugs is the rapid and extensive

* Corresponding author. Department of Pharmaceutics, Faculty of Pharmacy, Jamia Hamdard, Hamdard Nagar, New Delhi 110 062, India. Tel.: +91 11 2605 9688; fax: +91 11 2605 9663.
E-mail address: sanjay_bcp@rediffmail.com (S.K. Motwani).

0939-6411/$ - see front matter © 2007 Elsevier B.V. All rights reserved.
doi:10.1016/j.ejpb.2007.09.009

pre-corneal loss caused by the drainage and high tear fluid turnover [4,5]. Most efforts in ophthalmic drug delivery have been focused on increasing the corneal penetration of drugs with the final goal of improving the therapeutic outcome for treatments of different ocular diseases. These attempts include the use of colloidal drug delivery systems, such as liposomes [6], biodegradable nanoparticles [7] and nanocapsules [8]. However, the short residence time of these colloidal carrier systems in the ocular mucosa presents a major challenge for the therapy of extraocular diseases, such as keratoconjunctivitis sicca or dry eye disease. Consequently, the design of a mucoadhesive carrier system with improved drug delivery properties to the ocular surface would be a promising step towards the management of external ocular diseases.

Considering the fact that the cornea and conjunctiva have a negative charge, it was proposed that the use of mucoadhesive polymers, which may interact intimately with these extraocular structures, would increase the concentration and residence time of the associated drug. Among the wide variety of mucoadhesive polymers reported in the literature, the cationic polymer chitosan (CS) has been a polymer of choice because of its unique properties including acceptable biodegradability, biocompatibility [9–11] as well as the ability to increase membrane permeability, both *in vitro* [12–15] and *in vivo* [16] and be degraded by lysozymes in serum.

CS has been used in preparing films, beads, intragastric floating tablets, microspheres, and nanoparticles in the pharmaceutical field [17–22]. Also the CS has recently been proposed as a material with a good potential for ocular drug delivery as the CS solutions were found to prolong the corneal residence time of antibiotic drugs [23] and CS-coated nanocapsules were more efficient at enhancing the intraocular penetration of some specific drugs [24,25]. The interaction and prolonged residence time of CS nanoparticles at the ocular mucosa of rabbits have been reported and it was shown that following topical instillation of fluorescence-labelled nanoparticles, these colloidal drug carriers remain attached to the cornea and the conjunctiva for at least 24 h [26]. Therefore, mucoadhesive CS nanoparticles may have potential as colloidal drug delivery systems for the ocular mucosa.

Alginates are random, linear and anionic polysaccharides consisting of linear copolymers of α-L-guluronate and β-D-mannuronate residues. Alginates have a long history of use in numerous biomedical applications, including drug delivery systems, as they are biodegradable, biocompatible and mucoadhesive polymers [1]. Alginate polymers are also hemocompatible and have not been found to accumulate in any major organs and show evidence of *in vivo* degradation [27]. Sodium alginate (ALG) is used in a variety of oral and topical pharmaceutical formulations and it has been specifically used for the aqueous microencapsulation of drugs, in contrast to more conventional solvent-based systems [27,28].

The main objectives in drug delivery are to design systems that maintain the structure and activity of biomolecules; are non-immunogenic; release the therapeutic agent predictably over time; and degrade to non-toxic metabolites that are either absorbed or excreted [29]. A great deal of attention has been directed to polymeric colloidal nanoparticulate formulations obtained with polysaccharides, lipids and specifically natural biopolymers. The interaction between biodegradable cationic and anionic biopolymers leads to the formation of polyionic hydrogels, which have demonstrated favorable characteristics for drug entrapment and delivery. Chitosan and alginate are two biopolymers that have received much attention and have been extensively studied for such use [30]. Chitosan being a cationic polymer has been used for the production of microspheres and nanoparticles by ionotropic gelation with negatively charged polymers and there are many chitosan–polyanion complexes that have been investigated as drug delivery systems for drugs, proteins, DNA and other oligonucleotides, with encouraging results [31–36]. Among the various types of chitosan–polyanion complexes reported in the literature, the combination of chitosan and sodium alginate is considered to be the most interesting for colloidal carrier systems [37].

Chitosan–alginate (CS–ALG) polyionic complexes are formed through the ionic gelation via interactions between the carboxyl groups of alginate and the amine groups of chitosan. The complex protects the encapsulant, has biocompatible and biodegradable characteristics, and limits the release of encapsulated materials more effectively than either alginate or chitosan alone [38]. A further advantage of this delivery system is its non-toxicity permitting the repeated administration of therapeutic agents. CS–ALG microspheres or beads have been widely studied for the encapsulation of several drugs, proteins, cells and oligonucleotides, with promising results [37,39–43]. Despite the attractive properties offered by CS–ALG system, its development and application in the submicron scale has scarcely been studied [30,1].

In the present research, we report a slightly modified method to prepare CS–ALG nanoparticles based on the formation of a polyionic complex between the two biopolymers. The current study aimed at developing and optimising a mucoadhesive nanoparticulate formulation of gatifloxacin for ocular delivery using design of experiments by employing Box-Behnken statistical design.

2. Materials and methods

2.1. Materials

The polymer chitosan (CS) (specifications: molecular weight: 65–90 kDa, viscosity of 1% w/v aqueous solution in 2% v/v acetic acid: 130 mPa.s, deacetylation degree >80%) was received as a gift sample from India Sea Foods, India. The medium viscosity sodium alginate (ALG) isolated from *Macrocystis pyrifera*, having molecular weight

between 75 and 100 kDa, and mannuronic to guluronic acid ratio of 1.5 (60:40), was purchased from CDH Labs., India. Gatifloxacin was provided *ex gratia* by Lupin Labs Ltd., India. HPLC grade solvents were purchased from E. Merck (India) Ltd. Pluronic F127 was kindly provided by BASF Corporation, USA. Ultrapure water was obtained with MilliQ equipment (Waters, USA). All other solvents and materials used were of analytical grade.

2.2. Methods

2.2.1. Preparation of buffer solutions

The composition of artificial tear fluid (ATF), pH 7.4, was: sodium chloride 0.670 g, sodium bicarbonate 0.200 g, calcium chloride. $2H_2O$ 0.008 g, and purified water q.s. 100 g [43].

The composition of phosphate-buffered saline (PBS), pH 7.4, was: disodium hydrogen phosphate 1.38 g, potassium dihydrogen phosphate 0.19 g, sodium chloride 8.0 g, and purified water q.s. 1000 mL [44].

2.2.2. Preparation of chitosan–sodium alginate nanoparticles

Both the sodium alginate and chitosan solutions were prepared by dissolving the polymers in distilled water. The pH of the sodium alginate solutions (5.0–5.3) was adjusted using hydrochloric acid. The chitosan solutions were prepared using a previously published method, adjusting the amount of chitosan used to yield the desired concentration [30,45]. Briefly, a known amount of chitosan was dissolved in a solution of 1 M HCl, volume adjusted using distilled water and pH modified to 5.5–5.7 using 0.1 M NaOH. The sodium alginate and chitosan solutions were filtered under vacuum before use in nanoparticles preparation.

The CA–ALG nanoparticles were prepared by a modified coacervation method as reported by Calvo et al. [24,46]. Briefly, the aqueous solution of sodium alginate was sprayed into the chitosan solution containing Pluronic F-127 (0.5% w/v) under continuous magnetic stirring at 1000 rpm for 30 min. Pluronic F127 (0.50% w/v) was added to aid in solubilisation of gatifloxacin. Nanoparticles were formed as a result of the interaction between the negative groups of ALG and the positively charged amino groups of CS (ionotropic gelation). Nanoparticles were collected by centrifugation (REMI high speed, cooling centrifuge, REMI Corporation, India) at 18,000 rpm for 30 min at 4 °C. For particle size and size distribution study these nanoparticles were redispersed in 5 ml of ultrapure water.

Different mucoadhesive CS–ALG nanoparticulate formulations of gatifloxacin were prepared using the following composition: CS (0.10–0.30% w/v), ALG (0.20–0.60% w/v), gatifloxacin (0.01–0.10% w/v) and Pluronic F127 (0.50% w/v). Various formulations were prepared using the Box-Behnken experimental design.

The range of the two polymers under study was selected on the basis of preliminary experimentation where three kinds of phenomenon were observed: almost clear solutions, opalescent suspensions and aggregates. The zone of opalescent suspensions was of our interest for preparing mucoadhesive nanoparticulate systems and it was further examined and optimised using design of experiments i.e. Box-Behnken statistical design.

2.2.3. Experimental design

Use of experimental design allows for testing a large number of factors simultaneously and precludes the use of a huge number of independent runs when the traditional step-by-step approach is used. Systematic optimisation procedures are carried out by selecting an objective function, finding the most important or contributing factors and investigating the relationship between responses and factors by the so-called response surface methodology [47]. Objective function for the present study was selected as maximizing the % encapsulation efficiency while minimizing the particle size and % burst release.

Box-Behnken design was used to statistically optimise the formulation parameters and evaluate the main effects, interaction effects and quadratic effects of the formulation ingredients on the % encapsulation efficiency of mucoadhesive nanoreservoir systems. A 3-factor, 3-level design was used to explore the quadratic response surfaces and for constructing second order polynomial models using Design Expert® (Version 7.0.0, Stat-Ease Inc., Minneapolis, MN). The Box-Behnken design was specifically selected since it requires fewer runs than a central composite design, in cases of three or four variables [48]. This cubic design is characterised by set of points lying at the midpoint of each edge of a multidimensional cube and center point replicates ($n = 3$) whereas the 'missing corners' help the experimenter to avoid the combined factor extremes. This property prevents a potential loss of data in those cases [49]. A design matrix comprising of 15 experimental runs was constructed, for which the non-linear computer generated quadratic model is defined as;

$$Y = b_0 + b_1X_1 + b_2X_2 + b_3X_3 + b_{12}X_1X_2 + b_{13}X_1X_3 + b_{23}X_2X_3 + b_{11}X_1^2 + b_{22}X_2^2 + b_{33}X_3^2$$

where Y is the measured response associated with each factor level combination; b_0 is an intercept; b_1 to b_{33} are regression coefficients computed from the observed experimental values of Y from experimental runs; and X_1, X_2 and X_3 are the coded levels of independent variables. The terms X_1X_2 and X_i^2 ($i = 1$, 2 or 3) represent the interaction and quadratic terms, respectively [48–50].

Independent variables studied were the amount of the bioadhesive polymers: CS (X_1), ALG (X_2) and the amount of drug in the formulation (X_3). The dependent variables were the particle size (Y_1), zetapotential (Y_2), encapsulation efficiency (Y_3) and burst release (Y_4) with constraints applied on $Y_2 \geqslant 30$ mV for the long-term stability of nanoparticulate suspensions. The concentration range of independent variables under study is shown in Table 1 along with their low, medium and high levels, which were

Table 1
Variables in Box-Behnken design

Factor	Levels used, Actual (coded)		
	Low (−1)	Medium (0)	High (+1)
X_1 = Chitosan (% w/v)	0.10	0.20	0.30
X_2 = Sodium alginate (% w/v)	0.20	0.40	0.60
X_3 = Gatifloxacin (% w/v)	0.01	0.055	0.10
Dependent variables	Constraints		
Y_1 = Particle size (nm)	Minimize		
Y_2 = Zetapotential (mV)	$Y_2 \geqslant 30$		
Y_3 = Encapsulation efficiency (%)	Maximize		
Y_4 = Burst release (%)	Minimize		

selected based on the results from preliminary experimentation. The concentration of CS (X_1), ALG (X_2) and gatifloxacin (X_3) used to prepare the 15 experimental formulations and the corresponding observations for dependent variables are given in Table 2.

2.3. Characterisation of nanoparticles

2.3.1. Nanoparticles morphology

Morphological analysis of the chitosan nanoparticles was performed using transmission electron microscopy (TEM, Philips CM-10, USA). Samples of the nanoparticles suspension (5–10 μL) were dropped onto Formvar-coated copper grids. After complete drying, the samples were stained using 2% w/v phosphotungstic acid. DigitalMicrograph and Soft Imaging Viewer software were used to perform the image capture and analysis, including particle sizing.

Atomic force microscopy (AFM) was used to study the surface morphology and three-dimensional organisation and/or association of the nanoparticles. Nanoparticles suspension was diluted tenfold with ultrapure water and a drop was deposited on a glass thin layer fixed on a metallic magnetic support. The drop was dried overnight. The AFM images were collected with a NanoScope III (Digital Instruments, Santa Barbara, USA) operating in tapping mode.

2.3.2. Nanoparticles size and surface charge

Dynamic light scattering (DLS) (Brookhaven Instruments Corporation, Holtsville, NY) was used to measure the average nanoparticles size and size distribution (polydispersity index). All DLS measurements were done with a wavelength of 532 nm at 25 °C with an angle detection of 90°. Sample volume used for the analysis was kept constant i.e. 5 ml to nullify the effect of stray radiations from sample to sample. The zetapotential of nanoparticles was measured on a zetapotential analyzer (Zeecom, Japan). For zetapotential measurements, samples were diluted with 0.1 mM KCl and placed in the electrophoretic cell. All measurements were performed in triplicate ($n = 3$) and the standard deviation (SD) was recorded.

2.3.3. Fourier transform infra-red spectroscopy (FT-IR)

CS–ALG nanoparticles separated from nanoparticulate suspensions were dried by a freeze dryer, and their FT-IR transmission spectra were obtained using a FT-IR-8300 spectrophotometer (Shimadzu, Japan). A total of 2% (w/w) of sample, with respect to the potassium bromide (KBr; S.D. Fine Chem Ltd., Mumbai, India) disc, was mixed with dry KBr. The mixture was ground into fine powder using an agate mortar before compressing into KBr disc under a hydraulic press at 10,000 psi. Each KBr disc was scanned at 4 mm/s at a resolution of 2 cm over a wavenumber region of 400–4000 cm^{-1} using IRsolution software (ver. 1.10). The characteristic peaks were recorded for different samples.

Table 2
Observed responses in Box-Behnken design for gatifloxacin polymeric nanoparticles

Batch	Dependent variables			Independent variables				Burst release rate (mgh^{-1}) upto 15 min (Mean ± SEM)
	X_1 (%)	X_2 (%)	X_3 (%)	Y_1 (nm) (Mean ± SD)	Y_2 (mV) (Mean ± SD)	Y_3 (%) (Mean ± SD)	Y_4 (%) (Mean ± SD)	
1	0.10	0.20	0.06	205 ± 16	27.3 ± 3.9	77.67 ± 4.69	23.37 ± 3.29	9.27 ± 0.811
2	0.30	0.20	0.06	468 ± 23	47.8 ± 4.9	61.31 ± 4.07	14.63 ± 3.04	5.81 ± 0.723
3	0.10	0.60	0.06	273 ± 19	17.6 ± 3.1	71.82 ± 3.18	19.32 ± 4.16	7.67 ± 0.278
4	0.30	0.60	0.06	572 ± 27	38.1 ± 4.3	68.51 ± 5.11	11.45 ± 2.93	4.54 ± 0.509
5	0.10	0.40	0.01	243 ± 18	21.9 ± 3.4	74.53 ± 2.83	21.17 ± 3.67	8.40 ± 0.219
6	0.30	0.40	0.01	483 ± 24	42.2 ± 3.9	63.29 ± 2.47	13.71 ± 2.54	5.43 ± 0.347
7	0.10	0.40	0.10	261 ± 21	20.5 ± 2.9	76.84 ± 4.58	21.89 ± 3.32	8.69 ± 0.338
8	0.30	0.40	0.10	528 ± 23	42.3 ± 4.7	67.08 ± 3.77	13.02 ± 2.86	5.17 ± 0.320
9	0.20	0.20	0.01	338 ± 17	39.6 ± 4.1	62.54 ± 3.20	19.08 ± 3.59	7.57 ± 0.361
10	0.20	0.60	0.01	389 ± 21	30.2 ± 3.8	66.91 ± 5.34	11.93 ± 3.18	4.73 ± 0.098
11	0.20	0.20	0.10	391 ± 25	37.8 ± 3.5	64.43 ± 4.74	18.83 ± 2.97	7.47 ± 0.202
12	0.20	0.60	0.10	409 ± 22	30.8 ± 4.1	68.22 ± 2.61	12.23 ± 3.66	4.85 ± 0.304
13[a]	0.20	0.40	0.06	317 ± 20	34.7 ± 4.3	81.48 ± 5.03	14.78 ± 4.20	5.86 ± 0.267
14[a]	0.20	0.40	0.06	298 ± 18	33.1 ± 4.7	77.67 ± 4.85	14.26 ± 3.83	5.66 ± 0.412
15[a]	0.20	0.40	0.06	317 ± 21	35.5 ± 3.8	82.56 ± 3.57	13.46 ± 4.74	5.34 ± 0.329

[a] Indicates the center point of the design.

2.3.4. Differential scanning calorimetry

Differential scanning calorimetric (DSC) analysis was used to characterise the thermal behavior of the individual polymers and gatifloxacin, empty and gatifloxacin-loaded nanoparticles. DSC thermograms were obtained using an automatic thermal analyzer system (Pyris 6 DSC, Perkin-Elmer, USA). Temperature calibration was performed using Indium Calibration Reference Standard (transition point: 156.60 °C) as a standard. Samples were crimped in standard aluminum pans and heated from 40 to 400 °C at a heating rate of 10 °C/min under constant purging of dry nitrogen at 30 mL/min. An empty pan, sealed in the same way as the sample, was used as a reference.

2.3.5. Gatifloxacin loading of nanoparticles

The encapsulation efficiency of nanoparticles was determined by the separation of drug-loaded nanoparticles from the aqueous medium containing non-associated gatifloxacin by ultracentrifugation (REMI high speed, cooling centrifuge, REMI Corporation, India) at 18,000 rpm at 4 °C for 30 min. The amount of gatifloxacin loaded into the nanoparticles was calculated as the difference between the total amount used to prepare the nanoparticles and the amount that was found in the supernatant. The amount of free gatifloxacin in the supernatant was measured by a validated and stability-indicating HPTLC method using *n*-propanol–methanol–concentrated ammonia solution (25%) (5:1:0.9 v/v/v) as mobile phase [51]. The gatifloxacin encapsulation efficiency (EE) of the nanoparticles was determined in triplicate and calculated as follows [26,52]:

$$\text{Encapsulation Efficiency (EE)} = \frac{\text{Total gatifloxacin} - \text{Free gatifloxacin}}{\text{Total gatifloxacin}} \times 100.$$

2.3.6. In vitro release studies

In vitro release profiles of gatifloxacin from nanoparticles were determined as follows. The gatifloxacin-loaded CS–ALG nanoparticles were separated from the aqueous nanoparticulate suspension medium through ultra centrifugation. These nanoparticles were dried at 60 °C for 24 h in vacuum. Quantity of dried nanoparticles equivalent to about 20 mg of gatifloxacin was then re-dispersed in 5 mL of ultrapure water and placed in a dialysis membrane bag with a molecular cut-off of 5 kDa, tied and placed into 50 mL of dissolution media. The entire system was kept at 37° ± 0.5 °C with continuous magnetic stirring (25 rpm) and the study was carried out in two dissolution media: phosphate-buffered solution (PBS), pH 7.4 and artificial tear fluid (ATF), pH 7.4. At appropriate time intervals, 3 mL of the release medium was removed and 3 mL fresh medium was added into the system to maintain sink conditions. The amount of gatifloxacin in the release medium was evaluated by validated and stability-indicating HPTLC method [51]. The cumulative % drug release was calculated for the formulations and the drug release data were curve fitted using PCP Disso v2.08 software (Poona College of Pharmacy, Pune, India) to study the possible mechanism of drug release from mucoadhesive CS–ALG nanoreservoir systems. All measurements were performed in triplicate ($n = 3$) and the SD was calculated.

To evaluate the sustained release potential of mucoadhesive gatifloxacin-loaded CS–ALG nanoreservoir systems, the *in vitro* release profile of the marketed gatifloxacin ocular solution (Gatikind DPS, Mankind Pharma, India) was also determined under similar conditions and was used as a reference.

2.3.7. Optimisation data analysis and model-validation

ANOVA provision available in the software was used to establish the statistical validation of the polynomial equations generated by Design Expert®. A total of 15 runs with triplicate center points were generated by Box-Behnken design. All the responses observed were simultaneously fitted to first order-, second order- and quadratic-models and were evaluated in terms of statistically significant coefficients and R^2 values.

Various feasibility and grid searches were conducted over the experimental domain to find the compositions of the optimised nanoparticulate formulations. Three-dimensional response surface plots were provided by the Design Expert® software, where by intensive grid search performed over the whole experimental region, five optimum checkpoint formulations were selected to validate the chosen experimental domain and polynomial equations. The optimised checkpoint formulations were prepared and evaluated for various response properties. The resultant experimental values of the responses were quantitatively compared with that of the predicted values to calculate the percentage prediction error. Also, linear regression plots between actual and predicted values of the responses were produced using MS-Excel.

2.3.8. Freeze-drying and redispersibility of nanoparticles suspensions

Aliquots of six different batches of the optimised formulation were freeze-dried to study the physical stability of dried nanoparticles and the nanoparticles suspensions following redispersion. Mannitol (5% w/v) was added as a cryoprotectant to 50 mL aliquots of samples, which were frozen in liquid nitrogen and lyophilised (Heto Drywinner, Thermo Scientific, USA) for 48 h at 120 °C, at a 0.05 mmHg pressure. Freeze-dried samples, stored at room temperature, were rehydrated with the original volume of ultrapure water to restore the drug and polymer concentrations at every 2 months interval. The particle size, polydispersity index and zetapotential changes were assessed as described in Section 2.3.2. Reconstituted samples were also evaluated for any change in *in vitro* release profiles as described in Section 2.3.6.

3. Results and discussion

3.1. Formation and characterisation of gatifloxacin-loaded nanoparticles

The preparation of CS–ALG nanoreservoir systems, based on an ionotropic gelation process, involves mixing the two aqueous phases at room temperature. Because of the higher viscosity of CS solution, a number of experiments were performed by varying the concentration of CS and ALG, in order to screen the appropriate concentration range so as to allow the formation of turbid solutions and not the aggregates. The final concentration range selected for optimisation study was 0.10–0.30% w/v and 0.20–0.60% w/v for CS and ALG, respectively. The gatifloxacin concentration range selected was from 1:1 to 1:10 with respect to chitosan.

Recently, Douglas and Tabrizian [30] have studied the effect of pH on nanoparticles formation. They have demonstrated that an ALG solution of pH 5.3 generally produces smaller particle sizes when combined with high molecular weight CS (pH 5.5). It can be explained by the fact that as CS is poorly water soluble at neutral or alkaline pH, its solution is prepared under acidic conditions. CS is likely to precipitate out from solution upon addition of an ALG solution with higher pH resulting in less CS available for nanoparticles formation. Also as the pK_a of CS is reported to be 6.5 [53], an ALG solution of neutral pH, upon addition, would result in the majority of amine groups of CS being unprotonated and, therefore, unable to participate in ionic interactions with ALG. Using an ALG solution with a slightly lower pH (5.0–5.3) resolves these problems by allowing a stronger interaction between CS and ALG, leading to the formation of more compact and smaller nanoparticles. Additional studies, carried out in our laboratory ($n = 3$), in the more acidic pH range reveal that the use of acidified ALG (pH 2.2) or CS (pH 0.3) results in increased particle sizes and smaller CS–ALG nanoparticles are obtained when both the CS and ALG solutions have a pH in the range of 5.1–5.7. Within this range, the amine groups of the CS are protonated and the carboxyl groups of the ALG are ionised, which is most important for optimum interaction and the polyionic complex formation [30,54].

The observations for the particle size (nm), zetapotential (mV), encapsulation efficiency (%) and burst release (%) are presented in Table 2. It can be observed that the nanoparticles size, as previously reported by Calvo et al. [46], is dependent upon the concentration of two polymers (CS and ALG), the minimum size i.e. 205 nm (polydispersity 0.362), corresponding to the lowest CS and ALG concentration and the maximum size i.e. 572 nm (polydispersity 0.407), corresponding to the highest CS and ALG concentrations. These results confirm that smaller nanoparticles result, when the availability of the functional groups on two polymers for interaction is in stoichiometric proportion. On the other hand, the zetapotential of the nanoparticles was primarily affected by the CS concentration and was observed in the range of 17–27, 30–39 and 38–47 mV for the CS concentration of 0.10%, 0.20% and 0.30% w/v. It can be ascribed to the higher availability of protonated amine groups with increasing CS concentration.

As shown in Table 2, encapsulation efficiency of the nanoparticles was found to vary between 61% and 82%. It was also observed that the encapsulation of gatifloxacin into CS–ALG nanoparticles was highest (77–82%) when the CS, ALG and the drug were used at intermediate concentrations, whereas the encapsulation was found to be less than 70% when either of the CS or ALG is used at higher concentration levels. Also, there existed an inverse relationship between the particle size and gatifloxacin encapsulation which can be explained on the basis of the fact that at higher concentrations of the two polymers, it is polymers that make the bulk of the nanoparticles matrix and less volume is available for drug encapsulation.

3.2. Nanoparticles morphology

With TEM studies, the nanoparticles were seen to be distinct, spherical particles with solid dense structure (Fig. 1). Nanoparticles appeared to be considerably smaller when viewed with TEM as compared to the average particle size observed with DLS. Depending on the experimental

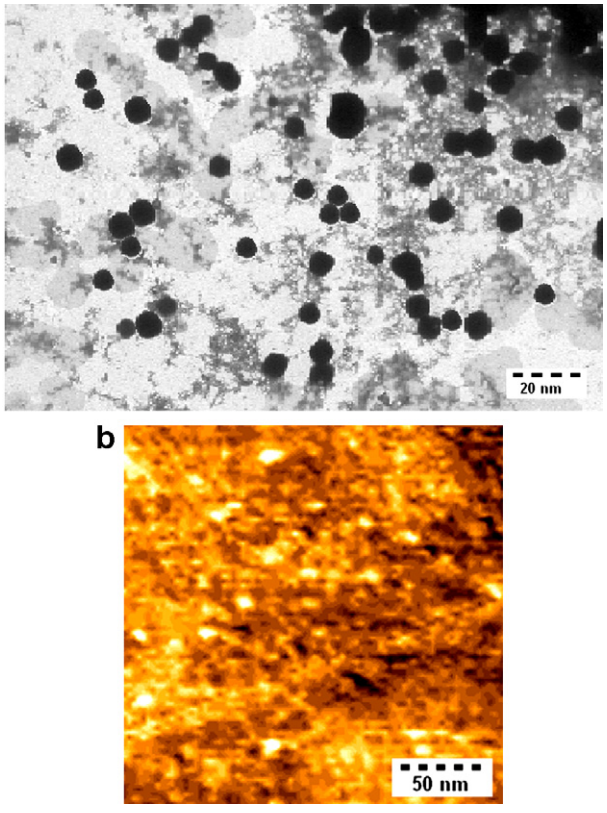

Fig. 1. (a) TEM photomicrograph of gatifloxacin-loaded CS–ALG nanoparticles. (b) AFM photomicrograph of gatifloxacin-loaded CS–ALG nanoparticles.

parameters used to prepare the nanoparticles, TEM images showed the nanoparticles sizes between 62 nm and 193 nm, whereas DLS sizing indicated that the smallest population has an average diameter of at least 379 nm. This apparent discrepancy between the two results can be explained by the dehydration of the CS–ALG hydrogel nanoparticles during sample preparation for TEM imaging. Also DLS measures the apparent size (hydrodynamic radius) of a particle, including hydrodynamic layers that form around hydrophilic particles such as those composed of CS–ALG, leading to an overestimation of nanoparticles size [55]. AFM studies also confirmed the presence of spherical and dense solid nanoparticles (Fig. 1) and three-dimensional view of the nanoparticles showed that the nanoparticles are discrete, which may be due to the presence of positive surface charge.

3.3. Identification of nanoparticles constituents

CS, ALG and CS–ALG nanoparticles were analysed using FT-IR spectrophotometer for characteristic absorption bands, indicative of their interaction. The peak at $\sim$1640 cm^{-1} in both the CS and CS–ALG nanoparticles spectra was due to the unreacted $–NH_2$ groups of CS. Similarly, peaks observed at $\sim$820 cm^{-1} and $\sim$1320 cm^{-1} in FT-IR spectra of ALG and CS–ALG nanoparticles represent unreacted –COOH groups of ALG. The characteristic peak observed at 1447 cm^{-1} (salt of carboxyl group) in the FT-IR spectrum of nanoparticles was attributed to the ionic interaction between these two reactive groups [56].

DSC thermograms of the CS, ALG and gatifloxacin showed characteristic endothermic peaks at 92.2 °C, 103.5 °C and 190.6 °C, respectively. The characteristic peak for gatifloxacin was found to be reduced in intensity and shifted to 184.3 °C, probably because of encapsulation in CS–ALG nanoparticles. Also two characteristic exothermic peaks, each for the CS and ALG, at 306.4 °C, 380.7 °C and 250.1 °C, 260.8 °C, respectively, disappear and could not be seen in CS–ALG nanoparticles.

3.4. Fitting of data to the model

There existed a direct relationship between the particle size and the polymer concentrations and at a constant concentration of 0.10% w/v of CS, the particle size of the nanoparticles was found to vary between 205 nm and 271 nm depending upon the ALG concentration. At 0.20% and 0.30% w/v concentration of CS the nanoparticles size varied between 300 nm and 410 nm and >450 nm, respectively, depending upon the concentration of ALG (Table 2).

Stability of nanoparticulate suspensions has always been a critical determinant for making the use of these suspensions, a viable alternative to the conventional ophthalmic delivery systems. It has been reported that the value of zetapotential less than −30 mV or higher than +30 mV can be used to assure the stability of nanoparticulate suspensions [57]. Zetapotential of the CS–ALG nanoreservoir systems was dependent upon the availability of total protonated $–NH_2$ group on CS and its neutralisation with $–COO^-$ groups of ALG. Higher the availability of $–NH_2$ groups (at higher CS concentration) and lower the neutralisation of these with $–COO^-$ groups (at lower concentration of ALG), higher was the zetapotential. Maximum zetapotential of 47.8 mV was observed at CS and ALG concentration of 0.30% and 0.20% w/v. It is also clear that the minimum concentration of CS i.e. 0.10% w/v is not suf-

Table 3
Summary of results of regression analysis for responses Y_1, Y_2, Y_3 and Y_4

Models	R^2	Adjusted R^2	Predicted R^2	SD	% CV	Remarks
Response (Y_1)						
Linear model	0.9143	0.8909	0.8728	1.13	3.29	–
Second order	0.9189	0.8581	0.8056	2.74	8.12	–
Quadratic model	0.9913	0.9871	0.9808	2.18	2.37	Suggested
Response (Y_2)						
Linear model	0.9814	0.9763	0.9640	1.33	4.07	–
Second order	0.9818	0.9682	0.9197	1.54	4.71	–
Quadratic model	0.9957	0.9881	0.9707	0.94	2.88	Suggested
Response (Y_3)						
Linear model	0.7965	0.8041	0.7217	3.21	5.23	–
Second order	0.8103	0.8023	0.7827	4.38	6.70	–
Quadratic model	0.9931	0.9892	0.9751	2.01	2.84	Suggested
Response (Y_4)						
Linear model	0.8621	0.8245	0.8090	1.69	7.29	–
Second order	0.8661	0.7657	0.7559	1.96	8.12	–
Quadratic model	0.9921	0.9887	0.9841	1.11	3.09	Suggested

Regression equations of the fitted model[a]

$$Y_1 = 310.67 + 133.62X_1 + 30.12X_2 + 17.00X_3 + 9.00X_1X_2 + 6.75X_1X_3 - 8.25X_2X_3 + 32.92X_1^2 + 35.92X_2^2 + 35.17X_3^2$$

$$Y_2 = 33.67 + 10.50X_1 - 4.13X_2 - 0.13X_3 + 0.25X_1X_2 + 0.25X_1X_3 - 1.83X_1^2 + 0.42X_2^2 - 0.58X_3^2$$

$$Y_3 = 80.57 - 5.08X_1 + 1.19X_2 + 1.16X_3 + 3.26X_1X_2 + 0.37X_1X_3 - 0.15X_2X_3 - 2.92X_1^2 - 7.83X_2^2 - 7.22X_3^2$$

$$Y_4 = 14.17 - 4.12X_1 - 2.62X_2 + 0.22X_1X_2 - 0.35X_1X_3 + 0.14X_2X_3 + 2.48X_1^2 + 0.55X_2^2 + 0.80X_3^2$$

[a] Only the terms with statistical significance are included.

ficient to produce the required zetapotential of >+30 mV (Table 2).

Fitting of the data for observed responses to various models, it was observed that the best-fitted model for all the four dependent variables was quadratic model (Table 3). The values of the coefficients for CS, ALG and gatifloxacin relates to the effects of these factors and their comparative significance on the encapsulation efficiency of nanoparticulate systems (Table 4). Higher values of the standard error (SE) for coefficients indicate the quadratic (non-linear) nature of the relationship.

A positive value in regression equation for a response represents an effect that favors the optimisation (synergistic effect), while a negative value indicates an inverse relationship (antagonistic effect) between the factor and the response [48]. From Table 3, it is evident that all the three independent variables viz. the concentration of the two biopolymers and the drug have positive effects on the response Y_1 (particle size) whereas the response Y_2 (zetapotential) has inverse relationship with ALG and drug concentration. It is primarily CS concentration, which favors the response Y_2. As the effect of CS concentration on Y_1 was about 13-fold as compared to the effect on Y_2, the particle size and zetapotential can be tailor-made to suit the specifications for a particular drug delivery system. Response Y_4 (% burst release) was observed to be unaffected by drug concentration whereas it can be retarded by increasing CS or ALG concentration (inverse relationship) (Table 3). The CS concentration had a negative effect on the response Y_3 (encapsulation efficiency), as at higher concentrations, the CS led to the formation of aggregates upon addition of ALG.

Coefficients with more than one factor term or higher order terms in the regression equation represent the interaction terms or quadratic relationships, respectively. It also suggests the existence of non-linear relationship between the responses and the factors. When the factors are varied at different levels in a formulation or when more than one factors are changed simultaneously, a factor can produce different degree of response than predicted by regression equations. The interaction effect of X_1 and X_2 was favorable (positive) for all the four response but it was highest for Y_1 (about 2.75-fold to that on Y_3) and almost equal for responses Y_2 and Y_4. The interaction effect of X_1 and X_3 was favorable for the responses Y_1, Y_2, and Y_3 but it has inverse relationship with responses Y_4. Highest and positive quadratic effects of X_1, X_2 and X_3 were observed for the response Y_1, whereas the negative quadratic effects (highest) of X_2 and X_1 were seen for the responses Y_3 and Y_2, respectively.

In addition to the close agreement between the predicted and adjusted R^2 values for each response, the value of R^2 was also observed to be >0.99 (Table 3) for all the regression equations generated, suggesting the statistical validity and significance of these equations for optimisation of nanoreservoir systems.

Table 4
Quadratic model and the coefficients for the particle size, zetapotential, encapsulation efficiency and burst release from formulations

Term	Particle size (nm)			Zetapotential (mV)			Encapsulation efficiency (%)			Burst release (%)		
	Coefficient	SE	Range[a]	Coefficient	SE	Range[a]	Coefficient	SE	Range[a]	Coefficient	SE	Range[a]
Constant	310.67	11.42	281.30–340.03	33.67	0.54	32.27–35.06	80.57	1.16	77.58–83.56	14.17	0.64	12.51–15.82
CS	133.62	7.00	115.64–151.61	10.50	0.33	9.65–11.35	− 5.08	0.71	(−6.91) to (−3.25)	−4.12	0.39	(−5.13) to (−3.10)
ALG	30.12	7.00	12.14–48.11	−4.13	0.33	(−4.98) to (−3.27)	1.19	0.71	(−0.64) to 3.02	−2.62	0.39	(−3.64) to (−1.61)
Drug	17.00	7.00	(−0.98) to 34.98	−0.13	0.33	(−0.98) to 0.73	1.16	0.71	(−0.67) to 2.99	–	–	(−1.00) to 1.02
CS × ALG	9.00	9.89	(−16.43) to 34.43	0.25	0.47	(−0.96) to 1.46	3.26	1.01	0.67–5.85	0.22	0.56	(−1.21) to 1.65
CS × Drug	6.75	9.89	(−18.68) to 32.18	0.25	0.47	(−0.96) to 1.46	0.37	1.01	(−2.22) to 2.96	−0.35	0.56	(−1.78) to 1.08
ALG × Drug	−8.25	9.89	(−33.68) to 17.18	–	–	(−1.21) to 1.21	−0.15	1.01	(−2.73) to 2.44	0.14	0.56	(−1.29) to 1.57
CS × CS	32.92	10.30	6.45–59.39	−1.83	0.49	(−3.09) to (−0.58)	−2.92	1.05	(−5.61) to (−0.22)	2.48	0.58	(0.99) to 3.97
ALG × ALG	35.92	10.30	9.45–62.39	0.42	0.49	(−0.84) to 1.67	−7.83	1.05	(−10.52) to (−5.13)	0.55	0.58	(−0.94) to 2.04
Drug × Drug	35.17	10.30	8.70–61.64	−0.58	0.49	(−1.84) to 0.67	−7.22	1.05	(−9.91) to (−4.53)	0.80	0.58	(−0.69) to 2.29

[a] The range indicates the lower and upper value of coefficients at 95% confidence interval.

From these equations, it is quite clear that the encapsulation efficiency is primarily affected by the CS concentration. The effects of ALG and drug concentration are almost equal on encapsulation efficiency but it is positive in contrast to the effect of CS concentration.

3.5. Response-surface analysis

Three-dimensional response surface plots drawn for the graphical optimisation of gatifloxacin-loaded mucoadhesive nanoreservoir system are presented in Figs. 2–4, which are very useful to study the interaction effects of the independent variables on the responses. These types of plots are useful in study of the effects of two factors on the response at one time, when the third factor is kept at a constant level. All the relationships among the three variables were non-linear, and it was observed that at lower CS concentration, the encapsulation efficiency of nanoparticles increases with increasing concentrations of either ALG or drug up to intermediate concentrations. Very high concentrations of CS resulted in the formation of aggregates rather than nanoparticles, which is highly undesired. Higher concentrations of gatifloxacin result in lower encapsulation and major proportion is washed away in supernatant during separation of nanoparticles. For the stability of nanoparticulate suspensions, the required minimum value of zetapotential (more than +30 mV) can be achieved when the availability of positively charged $-NH_2$ groups on CS is higher or the neutralisation by $-COO^-$ groups is less. It was observed that the lowest CS concentration of 0.10% could produce zetapotential of only 27.3 mV, even at the lowest concentration of ALG (least neutralisation expected).

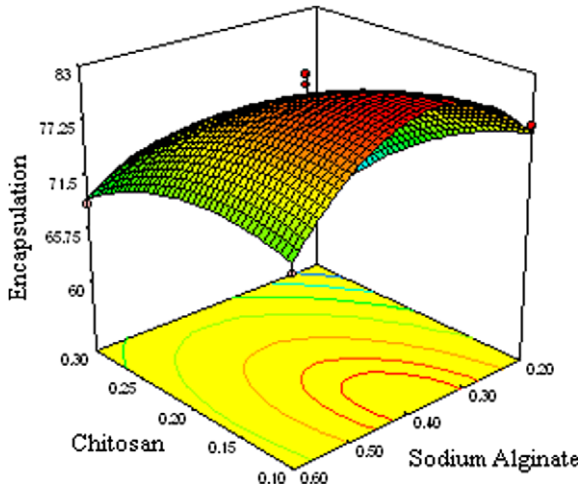

Fig. 2. Response surface plot showing effect of CS concentration (X_1) and ALG concentration (X_2) on % encapsulation efficiency (Y_3).

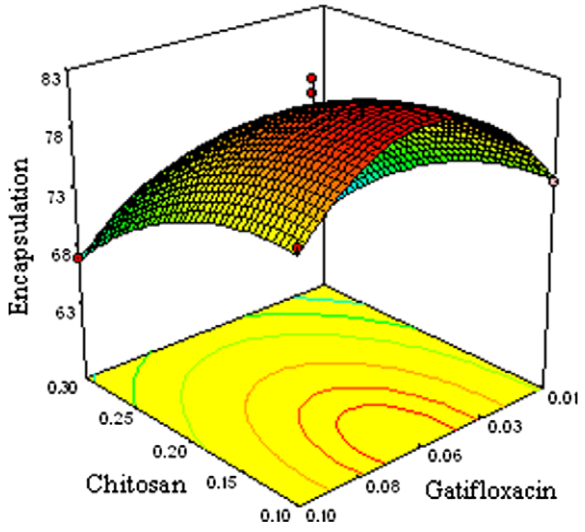

Fig. 3. Response surface plot showing effect of CS concentration (X_1) and gatifloxacin concentration (X_3) on % encapsulation efficiency (Y_3).

3.6. Optimisation

The optimum formulation of gatifloxacin-loaded CS–ALG nanoreservoir systems was selected based on the criteria of attaining the maximum value of encapsulation efficiency; minimizing the particle size and % burst release; and by applying constraints on $Y_2 \geqslant +30$ mV (Table 1). Upon 'trading of' various response variables and comprehensive evaluation of feasibility search and exhaustive grid search, the formulation composition with CS 0.22%, ALG 0.38% and gatifloxacin 0.05% was found to fulfill requisites of an optimum formulation. The optimised formulation has the encapsulation efficiency of 79.63% with particle size and zetapotential of 347 nm and +38.6 mV, respectively. The burst release from the optimised formulation was 11.08%.

3.7. In vitro release studies

The *in vitro* release study of the optimised formulation in ATF, pH 7.4 (Fig. 5) showed an initial burst release of

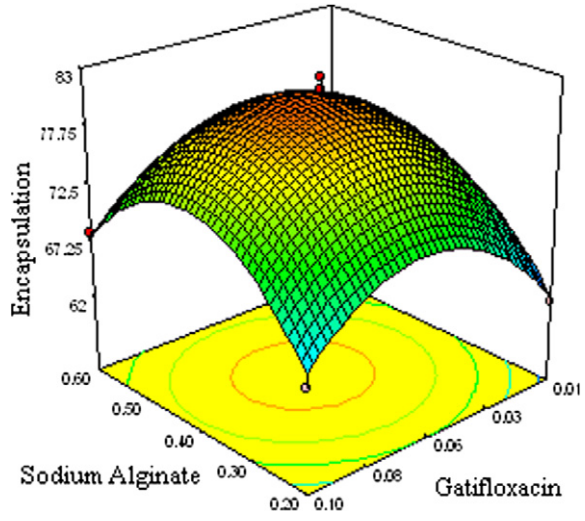

Fig. 4. Response surface plot showing effect of ALG concentration (X_2) and gatifloxacin concentration (X_3) on % encapsulation efficiency (Y_3).

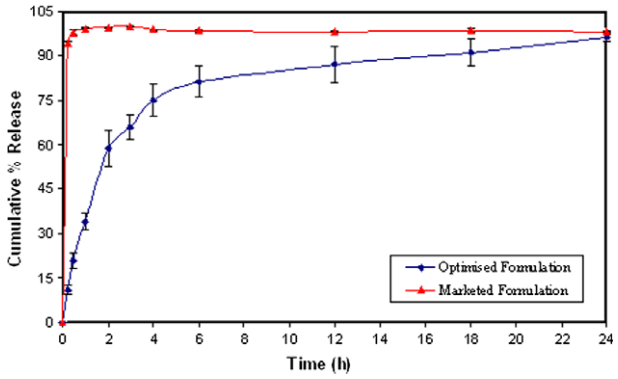

Fig. 5. *In vitro* release profiles of the optimised formulation of CS–ALG nanoparticles and marketed conventional formulation in ATF, pH 7.4.

about 10–12% of gatifloxacin, followed by a more gradual and sustained release phase for the following 24 h. Even after 24 h, about 5–7% of the drug still remained in the nanoparticles, regardless of the dissolution media used. When experiments were carried out in PBS, similar *in vitro* release profiles were observed (data not shown here) and there was no statistically significant difference (*t*-test, $p > 0.05$) between the release profiles of gatifloxacin from CS–ALG nanoparticles in PBS and ATF for the optimised formulation and the marketed formulation. Evaluation of the release profiles of the marketed conventional release formulation showed that almost all the gatifloxacin was released immediately after start of the study, suggesting that the developed nanoparticles can be used as an important platform for sustained drug release.

The initial fast release of gatifloxacin may be due to the rapid hydration of nanoparticles due to the hydrophilic nature of CS and ALG. The release medium penetrates into the particles and dissolves the entrapped gatifloxacin and, therefore, it could be proposed that the major factor determining the drug release from nanoparticles is its solubilisation or dissolution rate in the release medium. Further, it has been known that the solubility of gatifloxacin depends on pH (highest 40–60 mg/mL at pH 2–5) and its solubility at about physiological pH is very low (~10 mg/mL) [58,59]. In this sense, it is quite clear that the sink conditions in which this study was performed, and the extremely small size (large surface area) of the nanoparticles, account for the initial burst release. The absence of such a significant dilution process upon instillation into the eye suggests that this fast release should not occur *in vivo*.

Overall curve fitting (Table 5) showed that the drug release from mucoadhesive CS–ALG nanoparticles followed the zero-order model ($R^2 = 0.9972$) for burst release phase during first 15 min. Korsmeyer–Peppas model best described the sustained release phase ($R^2 = 0.9953$) during later 24 h with the critical value of n being 0.5817–0.7201 suggesting non-Fickian diffusion process. This is further supported by the fact that the sequential process of polymer hydration, solvent penetration, drug dissolution and/or polymer erosion determine the drug release from hydrophilic matrices [48,60].

3.8. Validation of RSM

For all of the five checkpoint formulations, the results of the evaluation for particle size, zetapotential, encapsulation efficiency and % burst release were found to be within limits (Table 6). Percentage prediction error helped in evaluating the validity of generated regression equations. Linear correlation plots between the actual and the predicted response variables (Fig. 6) showed the scatter of the residuals versus actual values to better represent the spread of the dependent variables under present experimental settings.

For validation of RSM results, the experimental values of the responses were compared with that of the anticipated values and the prediction error for the four response variables was found to vary between −2.88% and +2.52%. The linear correlation plots drawn between the predicted and experimental values demonstrated high values of R^2 (ranging between 0.9839 and 0.9957) indicating excellent goodness of fit ($p < 0.001$). Thus the low magnitudes of errors as well as the significant values of R^2 in the present investigation prove the high prognostic ability of the Box-Behnken designs.

3.9. Redispersibility of nanoparticles suspensions

For long-term storage of nanoparticles, aqueous solutions of the nanoparticles are essentially required to be lyophilised as solid products and it must be reconstituted into physiological solution as same as its original aqueous solution immediately before use [61–63].

Table 5
Dissolution model study by fitting *in vitro* release study[a]

Model	Equation	R^2 Value (15 runs) for burst release (%)	R^2 Value (15 runs) for sustained release (%)
Zero order	$m_o - m = kt$	0.9972 ± 0.0206	0.8763 ± 0.0291
First order	$\ln m = kt$	0.9301 ± 0.0156	0.9249 ± 0.0215
Higuchi's model	$m_o - m = kt^{1/2}$	0.9122 ± 0.0268	0.9548 ± 0.0326
Korsmeyer–Peppas	$\log (m_o - m) = \log K + n \log t$	0.9636 ± 0.0382	0.9953 ± 0.0188
Hixson–Crowell	$m_o^{1/3} - m^{1/3} = kt$	0.9470 ± 0.0296	0.9229 ± 0.0208

[a] m_0 is the initial drug amount (100%, when represented as percentage); m the amount of drug remaining at a specific time (calculated as % of m_0); k the rate constant; t is the time.

Table 6
Composition of checkpoint formulations, the predicted and experimental values of response variables and percentage prediction error

Optimised formulation composition (X_1:X_2:X_3)	Response variable	Experimental value	Predicted value	Percentage prediction error
0.17:0.43:0.06	Y_1 (nm)	281.00	283.89	−1.02
	Y_2 (mV)	31.3	30.53	+2.52
	Y_3 (%)	81.68	81.58	+1.28
	Y_4 (%)	15.01	15.11	−0.64
0.20:0.39:0.05	Y_1 (nm)	315.00	312.83	+0.69
	Y_2 (mV)	34.1	34.79	−1.98
	Y_3 (%)	79.13	79.76	−0.79
	Y_4 (%)	14.50	14.52	−1.03
0.21:0.37:0.06	Y_1 (nm)	323.00	326.87	−1.18
	Y_2 (mV)	34.4	35.42	−2.88
	Y_3 (%)	80.18	79.97	+0.26
	Y_4 (%)	13.96	13.83	+0.94
0.24:0.37:0.05	Y_1 (nm)	370.00	373.27	−0.87
	Y_2 (mV)	40.2	39.32	+2.24
	Y_3 (%)	77.89	77.79	+1.28
	Y_4 (%)	12.95	13.02	−0.51
0.26:0.35:0.05	Y_1 (nm)	403.00	399.17	+0.96
	Y_2 (mV)	39.7	40.16	−1.15
	Y_3 (%)	75.88	75.36	+0.69
	Y_4 (%)	13.67	13.69	−1.13

As the nanoparticles are presented with a tremendous increase in surface area and very high surface activity, aggregation and particle fusion are frequently noticed after a long period of storage of such nanoparticulate dispersions. Fig. 7 presents a change in particle size and zetapotential of reconstituted nanoparticles suspension, after storage for a period of 12 months at room temperature. These nanoparticles could be easily reconstituted by simple hand-agitation; however, it was observed that the average nanoparticles size was increased slightly with respect to the initial values, probably because of particles aggregation. Zetapotential values were found to be almost constant and it is proposed that a little increase in initial zetapotential values may further help in minimizing the particles aggregation by repulsion. Storage stability at room temperature revealed no significant changes in the *in vitro* release profiles of the gatifloxacin-loaded CS–ALG nanoparticles.

4. Conclusion

In the present study, the potential of CS–ALG nanoparticles as drug carriers for ocular delivery was investigated. Gatifloxacin, fourth generation fluoroquinolone, and a broad-spectrum antibacterial agent used in the treatment of ocular infections, was successfully formulated in the form of CS–ALG nanoreservoir system and the formulation was optimised by statistical screening design considering the concentration of chitosan, sodium alginate and gatifloxacin as independent variable. *In vitro* release studies

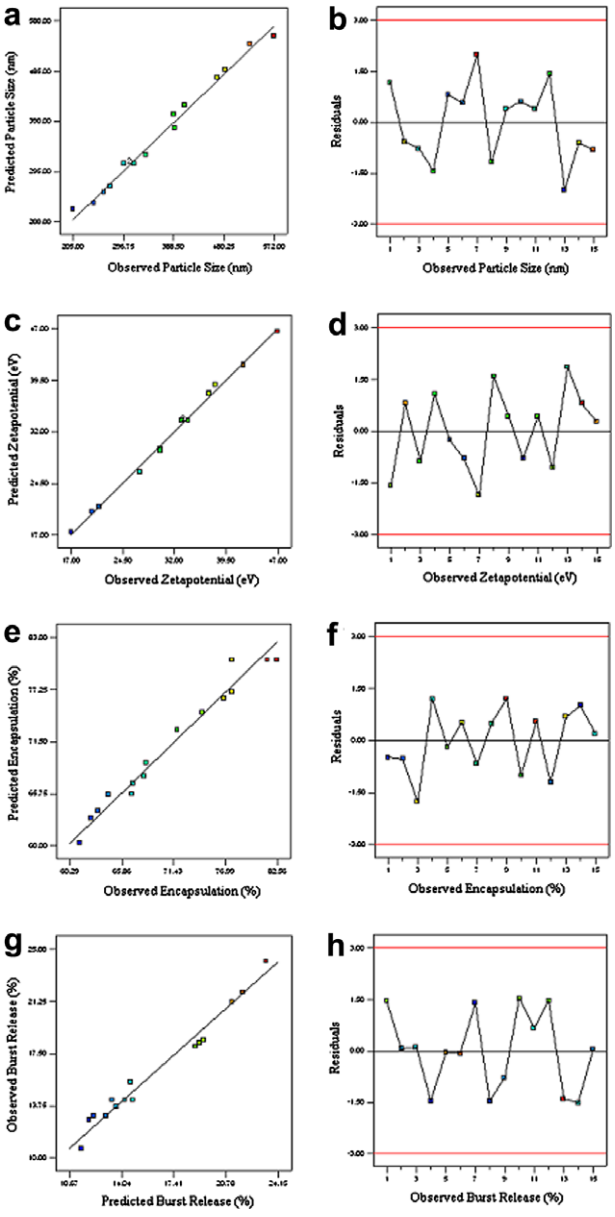

Fig. 6. Linear correlation plots (a, c, e, g) between actual and predicted values and the corresponding residual plots (b, d, f, h) for various responses.

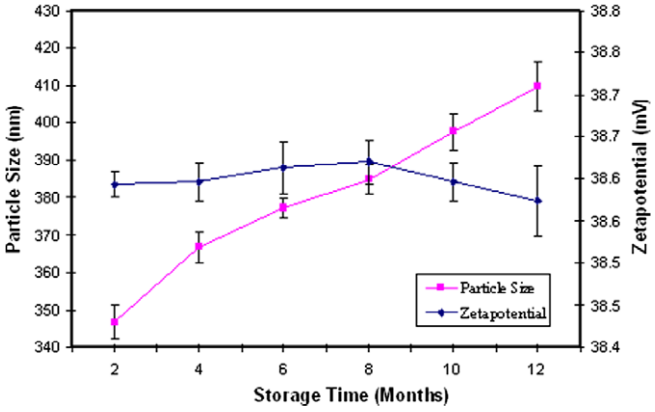

Fig. 7. Particle size and zetapotential of reconstituted optimised formulation upon storage for 12 months at room temperature.

showed that the drug is released from the optimised formulation over a period of 24 h in a sustained release manner, primarily by non-Fickian diffusion. This new formulation is a viable alternative to conventional eye drops by virtue of its ability to sustain the drug release, for its ease of administration because of reduced dosing frequency resulting in better patient compliance.

Acknowledgements

Authors wish to thank the Sophisticated Analytical Instruments Facilities (SAIF), AIIMS, New Delhi, India, for providing the facilities of TEM. Authors are grateful to Dr. Prasenjit Sen, Jawaharlal Nehru University, New Delhi, India, for providing the facilities of AFM.

References

[1] S. De, D. Robinson, Polymer relationships during preparation of chitosan–alginate and poly-L-lysine–alginate nanospheres, J. Control. Rel. 89 (2003) 101–112.
[2] R. Gref, Y. Minamitake, M.T. Perracchia, V. Trubeskoy, V. Torchilin, R. Langer, Biodegradable long-circulating polymeric nanospheres, Science 263 (1994) 1600–1603.
[3] M.J. Alonso, Nanomedicines for overcoming biological barriers, Biomed. Pharmacoth. 58 (2004) 168–172.
[4] J.C. Lang, Ocular drug delivery conventional ocular formulations, Adv. Drug Deliv. Rev. 16 (1995) 39–43.
[5] C. Le Bourlais, L. Acar, H. Zia, P.A. Sado, T. Needham, R. Leverge, Ophthalmic drug delivery systems: recent advances, Prog. Retinal Eye Res. 17 (1998) 33–58.
[6] G. Smolin, M. Okumoto, S. Feiler, D. Condon, Idoxuridine–liposome therapy for herpes simplex keratitis, Am. J. Ophthalmol. 91 (1981) 220–225.
[7] C. Losa, P. Calvo, E. Castro, J.L. Vila-Jato, M.J. Alonso, Improvement of ocular penetration of amikacin sulphate by association to poly(butylcyanoacrylate) nanoparticles, J. Pharm. Pharmacol. 43 (1991) 548–552.
[8] C. Losa, L. Marchal-Heussler, F. Orallo, J.L. Vila-Jato, M.J. Alonso, Design of new formulations for topical ocular administration: polymeric nanocapsules containing metipranolol, Pharm. Res. 10 (1993) 80–87.
[9] J. Knapczyk, L. Krowczynski, J. Krzck, M. Brzeski, E. Nirnberg, D. Schenk, H. Struszcyk, Requirements of chitosan for pharmaceutical and biomedical applications, in: G. Skak-Braek, T. Anthonsen, P. Sandford (Eds.), Chitin and Chitosan: Sources, Chemistry, Biochemistry, Physical Properties and Applications, Elsevier, London, 1989, pp. 657–663.
[10] S. Hirano, H. Seino, I. Akiyama, I. Nonaka, Chitosan: a biocompatible material for oral and intravenous administration, in: C.G. Gebelein, R.L. Dunn (Eds.), Progress in Biomedical Polymers, Plenum Press, New York, 1990, pp. 283–289.
[11] S. Hirano, H. Seino, Y. Akiyama, I. Nonaka, Biocompatibility of chitosan by oral and intravenous administration, Polym. Eng. Sci. 59 (1989) 897–901.
[12] P. Artursson, T. Lindmark, S.S. Davis, L. Illum, Effect of chitosan on the permeability of monolayers of intestinal epithelial cells (Caco-2), Pharm. Res. 11 (1994) 1358–1361.
[13] T.J. Aspden, J.D. Mason, N.S. Jones, Chitosan as a nasal delivery system: the effect of chitosan solutions on *in vitro* and *in vivo* mucociliary transport rates in human turbinates and volunteers, J. Pharm. Sci. 86 (1997) 509–513.
[14] C.M. Lehr, J.A. Bouwstra, E. Schacht, H.E. Junginger, *In vitro* evaluation of mucoadhesive properties of chitosan and some other natural polymers, Int. J. Pharm. 78 (1992) 43–48.
[15] S. Dumitriu, E. Chornet, Inclusion and release of proteins from polysaccharide-based polyion complexes, Adv. Drug Deliv. Rev. 31 (1998) 223–246.
[16] H. Takeuchi, H. Yamamoto, T. Niwa, T. Hino, Y. Kawashima, Enteral absorption of insulin in rats from mucoadhesive chitosan-coated liposomes, Pharm Res. 13 (1996) 896–901.
[17] A. Berthold, K. Cremer, J. Kreuter, Preparation and characterization of chitosan microspheres as drug carrier for prednisolone sodium phosphate as model for anti-inflammatory drugs, J. Control. Rel. 39 (1996) 17–25.
[18] O. Felt, P. Buri, R. Gurny, Chitosan: a unique polysaccharide for drug delivery, Drug Dev. Ind. Pharm. 24 (1998) 979–993.
[19] P. Giunchedi, I. Genta, B. Conti, R.A.A. Muzzarelli, U. Conte, Preparation and characterization of ampicillin loaded methylpyrrolidinone and chitosan microspheres, Biomaterials 19 (1998) 157–161.
[20] P. Calvo, C. Remunan-Lopez, J.L. Vila-Jato, M.J. Alonso, Chitosan and chitosan/ethylene oxide-propylene oxide block copolymernanoparticles as novel carriers for proteins and vaccines, Pharm. Res. 14 (1997) 1431–1436.
[21] L. Illum, Chitosan and its use as a pharmaceutical excipient, Pharm. Res. 15 (1998) 1326–1331.
[22] Y. Wu, Q. Wu, Y.N. Wang, J.B. Ma, Tautomerization of quercetin induced by chitosan, Acta Chim. Sin. 61 (2003) 614–618.
[23] O. Felt, P. Furrer, J.M. Mayer, B. Plazonnet, P. Buri, R. Gurny, Topical use of chitosan in ophthalmology: tolerance assessment and evaluation of pre-corneal retention, Int. J. Pharm. 180 (1999) 185–193.
[24] P. Calvo, J.L. Vila-Jato, M.J. Alonso, Evaluation of cationic polymer-coated nanocapsules as ocular drug carriers, Int. J. Pharm. 53 (1997) 41–50.
[25] I. Genta, B. Conti, P. Perugini, F. Pavaneto, A. Spadaro, G. Puglisi, Bioadhesive microspheres for ophthalmic administration of acyclovir, J. Pharm. Pharmacol. 49 (1997) 737–742.
[26] A.M. De Campos, A. Sánchez, M.J. Alonso, Chitosan nanoparticles: a new vehicle for the improvement of the delivery of drugs to the ocular surface. Application to cyclosporin A, Int. J. Pharm. 224 (2001) 159–168.
[27] M. Rajaonarivony, C. Vauthier, G. Couarraze, F. Puisieux, P. Couvreur, Development of a new drug carrier made from Alginate, J. Pharm. Sci. 82 (1993) 912–917.
[28] R. Bodmeier, J. Wang, Microencalpsulation of drugs with aqueous colloidal polymer dispersions, J. Pharm. Sci. 82 (1993) 191–194.
[29] T.P. Richardson, W.L. Murphy, D.J. Mooney, Crit. Rev. Eukaryot. Gene Expr. 11 (2001) 47–58.
[30] K.L. Douglas, M.J. Tabrizian, Effect of experimental parameters on the formation of alginate–chitosan nanoparticles and evaluation of their potential application as DNA carrier, J. Biomater. Sci. Polymer Edn. 16 (2005) 43–56.
[31] S.A. Agnihotri, N.N. Mallikarjuna, T.M. Aminabhavi, Recent advances on chitosan-based micro- and nanoparticles in drug delivery, J. Control. Rel. 100 (2004) 5–28.
[32] K.A. Janes, P. Calvo, M.J. Alonso, Polysaccharide colloidal particles as delivery systems for macromolecules, Adv. Drug Deliv. Rev. 47 (2001) 83–97.
[33] K.W. Leong, H.Q. Mao, L. Truong, K. Roy, S.M. Walsh, J.T. August, DNA-polycation nanospheres as non-viral gene delivery vehicles, J. Control. Rel. 53 (1998) 183–193.
[34] K.A. Janes, M.P. Fresneau, A. Marazuela, A. Fabra, M.J. Alonso, Chitosan nanoparticles as delivery systems for doxorubicin, J. Control. Rel. 73 (2001) 255–267.
[35] Y.J. Yuji, M.X. Xu, X. Chen, K.D. Yao, Drug release behavior of chitosan/gelatin network polymer microspheres, Chin. Sci. Bull. 41 (1996) 1266–1268.
[36] K.Y. Lee, I.C. Kwon, Y.H. Kim, W.H. Jo, S.Y. Jeong, Preparation of chitosan self aggregates as a gene delivery system, J. Control. Rel. 51 (1998) 213–220.
[37] F.-L. Mi, H.-W. Sung, S.-S. Shyu, Drug release from chitosan–alginate complex beads reinforced by a naturally occurring cross-linking agent, Carbohydr. Polym. 48 (2002) 61–72.

[38] X.L. Yan, E. Khor, L.Y. Lim, Chitosan-alginate films prepared with chitosans of different molecular weights, J. Biomed. Mater. Res. 58 (2001) 358–365.
[39] G. Coppi, V. Iannuccelli, E. Leo, M.T. Bernabei, R. Cameroni, Protein immobilization in crosslinked alginate microparticles, J. Microencapsul. 19 (2002) 37–44.
[40] M.L. Gonzalez-Rodriguez, M.A. Holgado, C. Sanchez-Lafuente, A.M. Rabasco, A. Fini, Alginate/chitosan particulate systems for sodium diclofenac release, Int. J. Pharm. 232 (2002) 225–234.
[41] S. Takka, F. Acarturk, Calcium alginate microparticles for oral administration. II. Effect of formulation factors on drug release and drug entrapment efficiency, J. Microencapsul. 16 (1999) 275–290.
[42] M.L. Huguet, E. Dellacherie, Ca-alginate beads coated with chitosan: effect of the structure of encapsulated materials on their release, Proc. Biochem. 31 (1996) 745–751.
[43] M.M. Van Ooteghem, in: P. Edman (Ed.), Biopharmaceutics of Ocular Drug Delivery, CRC Press, Boca Raton, 1993, pp. 27–41.
[44] Indian Pharmacopoeia, vol. 2, Ministry of Health and Family Welfare, Govt. of India, 1996, pp. A144.
[45] F. Chellat, M. Tabrizian, S. Dumitriu, E. Chornet, P. Magny, C.H. Rivard, L. Yahia, In vitro and *in vivo* biocompatibility of chitosan-xanthan polyionic complex, J. Biomed. Mater. Res. 51 (2000) 107–116.
[46] P. Calvo, C. Remunan-Lopez, J.L. Vila-Jato, M.J. Alonso, Novel hydrophilic chitosan-polyethylene oxide nanoparticles as protein carriers, J. Appl. Polym. Sci. 63 (1997) 125–132.
[47] L.V. Candioti, J.C. Robles, V.E. Mantovani, H.C. Goicoechea, Multiple response optimization applied to the development of a capillary electrophoretic method for pharmaceutical analysis, Talanta 69 (2006) 140–147.
[48] S. Chopra, G.V. Patil, S.K. Motwani, Release modulating hydrophilic matrix systems of losartan potassium: Optimisation of formulation using statistical experimental design, Eur. J. Pharm. Biopharm. 66 (2007) 73–82.
[49] S. Chopra, S.K. Motwani, Z. Iqbal, S. Talegaonkar, F.J. Ahmad, R.K. Khar, Optimisation of polyherbal gels for vaginal drug delivery by Box-Behnken statistical design, Eur. J. Pharm. Biopharm. 67 (2007) 120–131.
[50] G.E.P. Box, D.W. Behnken, Some new three level designs for the study of quantitative variables, Technometrics 2 (1960) 455–475.
[51] S.K. Motwani, R.K. Khar, F.J. Ahmad, S. Chopra, K. Kohli, S. Talegaonkar, Z. Iqbal, Stability indicating high-performance thin-layer chromatographic determination of gatifloxacin as bulk drug and from polymeric nanoparticles, Anal. Chim. Acta 576 (2006) 253–260.
[52] Y.W.W. Yang, C. Wang, J. Hu, S. Fu, Chitosan nanoparticles as a novel delivery system for ammonium glycyrrhizinate, Int. J. Pharm. 295 (2005) 235–245.
[53] H.Q. Mao, K. Roy, L. Troung, K.A. Janes, K.Y. Lin, Y. Wang, J.T. August, K.W. Leong, Chitosan-DNA nanoparticles as gene carriers: synthesis, characterization and transfection efficiency, J. Control. Rel. 70 (2001) 399–421.
[54] S. Dumitriu, P. Magny, D. Montane, P.F. Vidal, E. Chornet, Polyionic hydrogels obtained by complexation between Xanthan and Chitosan: Their properties as supports for enzyme immobilization, J. Bioact. Compat. Polym. 9 (1994) 184–209.
[55] S. Prabha, W.Z. Zhou, J. Panyam, V. Labhasetwar, Size-dependency of nanoparticle-mediated gene transfer: studies with fractionated nanoparticles, Int. J. Pharm. 244 (2002) 105–115.
[56] F.A. Simsek-Ege, G.M. Bond, J. Stringer, Polyelectrolyte complex formation between alginate and chitosan as a function of pH, J. Appl. Polym. Sci. 88 (2003) 346–351.
[57] Pharmaceutical Literature, Zetapotential: A complete course in 5 min, Zeta Meter Inc., Staunton, USA 2006. (http://www.zeta-meter.com).
[58] K. Inada, S. Yasueda, Aqueous liquid pharmaceutical composition comprised of gatifloxacin, US Patent No. 6,333,045, 2000.
[59] Tequin (Gatifloxacin) Tablets, www.rxlist.com/cgi/generic/gatifloxacin.htm.
[60] A.T. Pham, P.I. Lee, Probing the mechanism of drug release from hydroxypropylmethyl cellulose matrices, Pharm. Res. 11 (1994) 1379–1385.
[61] M. Chacon, J. Molpeceres, L. Berges, M. Guzman, M.R. Aberturas, Stability and freeze-drying of cyclosporine loaded poly (dl-lactide-glycolide) carriers, Eur. J. Pharm. Sci. 8 (1999) 99–107.
[62] F.D. Jaeghere, E. Allemann, J.C. Leroux, W. Stevels, J. Feijen, E. Doelker, R. Gurny, Formulation and lyoprotection of poly (lactic acid-co-ethylene oxide) nanoparticles: influence on physical stability and *in vitro* cell uptake, Pharm. Res. 16 (1999) 859–866.
[63] E. Zimmermann, R.H. Muller, K. Mader, Influence of different parameters on reconstitution of lyophilized SLN, Int. J. Pharm. 196 (2000) 211–213.